August 26, 2012

Subject: Chondrocyte model manuscript
From: Mary M Maleckar <mmaleck@simula.no>
Date: 8/24/2012 8:31 AM
To: Wayne Giles <wgiles@ucalgary.ca>
CC: Sheila Crombie <crombie@ucalgary.ca>

Dear Wayne,

Apologies for not sending this to you earlier; attached is a preliminary version of the chondrocyte manuscript for your perusal. I had wanted to flesh out the Results and take a first pass at the Discussion myself before sending. Since I wasn't able to work on this this week, my advance apologies for the lack of completeness in those sections.

Please feel free to forward any questions, and I look forward to discussing further.

Best wishes from Oslo,

Molly

Attachments:

chondrocyte-model.pdf 27 bytes

The Role of K^+ ~~channels~~ Currents in Human Articular Chondrocyte Electrophysiology: a Computational Perspective

Harish Narayanan[1]
Center for Biomedical Computing,
Simula Research Laboratory, Lysaker, Norway

Mary M. Maleckar,
Center for Biomedical Computing,
Simula Research Laboratory, Lysaker, Norway

Wayne R. Giles,
Faculty of Kinesiology,
University of Calgary, Calgary, Canada

22nd August 2012

Robert B. Clark
Faculty of Kinesiology
U of C

[1]Corresponding author. Address: Center for Biomedical Computing, Simula Research Laboratory, P.O. Box 134, 1325 Lysaker, Norway Tel.:+47 4003-4801, Fax: +47 6782-8201

Abstract

~~We present~~ a computational model for studying the electrophysiology of the human articular chondrocyte. ~~It is novel.~~ ~~We present some numerical results to help demonstrate aspects of the behaviour of the model. We pay particular attention to the potassium channels and the effect of blocking~~ $I_{K_{2\,pore}}$ ~~on the cell's RMP. This will serve as a useful tool in helping us understand the causes of osteoarthritis and things like the "frozen shoulder" syndrome.~~

Key words: chondrocyte; electrophysiology; potassium channels; computational model

Needs to be rewritten completely. For BioPhys J, the abstract takes the following form:

- One general intro sentence, setting up
- Problem statement
- What we are going to do about it (methods)
- What happened (results) (Most important)
- Conclusion

ToDo

We have developed a novel computational model based on experimental data which has identified the role of 2-pore K+ channel expression.

The utility of the model is illustrated by focusing on the role of a novel 2-pore K+ channel in regulating the resting potential and transepithelial ion ($e.g.\ Ca^{2+}$) homeostasis.

Good. Leave for Draft #2

Introduction

Articular cartilage is aneural, avascular, alymphatic, flexible connective tissue that covers the articulating ends of diarthroidal joints (1, 2) and permits stability and movement of the skeleton. This connective tissue consists of an extracellular matrix (ECM, composed primarily of collagen, elastin and proteoglycans, as detailed below) and one type of cell—the *chondrocyte*—which is responsible for synthesis and homeostasis of the matrix. Articular cartilage is regularly exposed to mechanical stresses, and this exposure is essential for the health of the tissue (3). Chondrocytes occupy only 1–10% of the total volume of articular cartilage in mammals (4, 5) and play no direct mechanical role. Instead, mechanical support is provided by the ECM, which is composed of (a) collagen fibers, which gives the tissue the ability to resist tension, (b) negatively-charged gel-like proteoglycans (PGs) trapped within the collagen mesh, allowing the tissue to bear compression (1, 6) and (c) synovial fluid within the articular capsule which acts as a lubricant, allowing for free movement of the bones (7). The chondrocyte thus resides in a physiologically atypical and dynamic environment and its primary role is to maintain viable cartilage by balancing macromolecular synthesis and breakdown (see e.g. Stockwell (3), Wilkins et al. (8), Fassbender (9)).

Under abnormal conditions, chondrocyte damage may occur and the balance between matrix synthesis and degradation is lost, causing inflammation of the tissue and/or osteoarthritis: a wearing out of the cartilage layer which causes painful, bone-against-bone friction. It is generally known that the progression of osteoarthritis (Rush and Hall, 2003) and limited recovery of chondrocytes (Jones et al, 1999) is linked to poorly-regulated volume changes (10); physical damage to cartilage is easier in the context of reduced osmolarity (Bushet et al, 2005). In turn, there is indication that these volume changes are linked to abnormal maintenance of resting membrane potential in these cells (10). In abnormal cells, the response to challenging external stimuli may be altered (e.g. much larger changes in resting membrane potential) as compared to healthy cells (Lewis et al, 2011; WIlson, et al 2004; Tsuga 2002; Tirabashi 2010a). It has been suggested that such changes in the regulation of the resting membrane potential are due to altered ion channel function (Lewis et al, 2011; WIlson, et al 2004; Tsuga 2002; Tirabashi 2010a). Direct experimental investigation of the link between chondrocyte electrophysiology and chondrotoxicity is complicated, however, by chondrocytes' small cell size and the associated limitations of in vitro electrophysiological studies. We have thus developed and present here a detailed, biophysically based model of chondrocyte electrophysiology. The

human

ion

As a result

thinning

What does this phrase mean?

more fragile

is likely

chondrocytes.

For the purpose of integrating available data and attempting to understand it functional significance.

~~first of its kind, the~~ model will facilitate investigation of questions related to chondrocyte electrophysiology, ~~and~~ signaling, ~~and provides a profound basis for subsequent models of~~ chondrocyte ~~and~~ articular pathophysiology.

Osteoarthritic changes may develop in even young patients following orthopedic surgery (cite) via chondrolysis, a condition in which accelerated loss of articular cartilage occurs over a short time period (Webb editorial, 2009). Several clinical studies have suggested that this significant chondrotoxicity can occur as a result of postoperative administration of bupivacaine, a local anesthetic (Busfield and Romero, 2009; Bailie and Ellenbecker, 2009; Rapley et al, 2009; Wiater, et al, 2011). Experimental work has confirmed that bupivacaine ~~reveals~~ profound chondrotoxic effects in both cell (11) and animal studies (Gomoll et al, 2006; Chu et al, 2010). The ~~exact~~ mechanisms leading to chondrotoxicity ~~in this context~~ remain unclear. ~~However, it appears that the mechanism of toxicity is unrelated to the primary mechanism of action of bupivacaine, the blockade of voltage-gated sodium channels (cite), and instead may be related to potassium channel blockade (Grishko, et al, 2010).~~ ~~Additionally, it is known that~~ the family of two-pore K+ channels, recently identified in human articular chondrocytes (Clark, et al, manuscript) ~~is likely affected by~~ bupivacaine ~~administration~~ (Clark et al, manuscript; Punke et al 2003). We therefore hypothesized that the blockade of the two-pore K+ channel in human articular chondrocytes by the local anesthetic bupivacaine leads to ~~abnormal~~ regulation of the resting membrane potential in these cells, ~~which may concomitantly lead to abnormal volume regulation, altered signaling, and cell death.~~ ~~This paper aims to~~ (1) ~~present~~ the first model of chondrocyte electrophysiology ~~in detail~~ and, (2) to use this model to investigate the potential role of bupivacaine in the homeostasis of the chondrocyte resting membrane potential ~~and subsequent volumetric changes.~~

Model and Methods

~~We focus our attention~~ on a single chondrocyte cell residing in deep regions of cartilage. This extracellular environment can be modelled ~~simply~~ by ~~fixing~~ external concentrations $[Na^+]_o$, $[K^+]_o$, $[Ca^{2+}]_o$, $[H^+]_o$ and $[Cl^-]_o$ within physiologically-relevant ranges (see Table 1). The chondrocyte cell membrane ~~boasts a host of~~ voltage- and ligand-gated ion channels as well as pumps and exchangers (12); the channels ~~under~~ under consideration in this model are illustrated in Figure 1 and described in the following section.

Ionic current formulations

> Needs some introductory text here. Point to the fact that the discussion contains other identified channels not explicitly modelled in this work.

ToDo

Potassium channels

Experimental results reported by Clark et al. (13) suggest that potassium channels play a dominant role in controlling the RMP of the human tibial joint articular chondrocyte. Motivated by these observations, our mathematical model incorporates the following three primary channels for potassium ion transport.

Two-pore potassium channels are a set of widely-expressed K^+-selective channels whose activation is largely independent of membrane potential. They appear to play a vital role in determining the RMP of the cell. Following Unknown (12), the mathematical expression used to compute this current is:

$$I_{\mathrm{K_{2\,pore}}} = P_{\mathrm{K}} \frac{z_{\mathrm{K}}^2 V F^2}{RT} \frac{([K^+]_i - [K^+]_o \exp(\frac{-z_{\mathrm{K}} V F}{RT}))}{(1 - \exp(-z_K V F/(RT)))}, \qquad (1)$$

and Figure 2a shows the voltage-current curve for this channel fit to experimental data.

Several experimental studies point to the existence of (large) **calcium-activated potassium** channels (14). Such channels are hypothesised to act as "osmolytic channels," responsible for decreasing intracellular osmotic potential by fostering efflux of potassium ions. This affects the ability of the chondrocyte to regulate its volume under rapid changes in physiochemical environment (10). In addition, studies suggest (12) that this channel can be stretch-activated (stretch causes an increase in calcium influx, which results in markedly increased potassium current).

In the present formulation, we ignore the stretch dependence and model the (large) calcium-activated potassium channel using a functional form defined by Horrigan and Aldrich (15):

$$I_{\mathrm{K_{Ca-act}}} = N_{\mathrm{K_{Ca-act}}} P_0 G_{\max} (V - E_{\mathrm{K}}), \qquad (2)$$

where,

$$
\begin{aligned}
kTe &= 23.54\,(T/273),\\
L_v &= L0\,\exp((V\,Z_L)/kTe),\\
J_v &= \exp(((V - Vh_j)\,Z_j)/Kate),\\
K &= Ca_i/KDc,\\
P_0 &= \frac{L_v\,(1 + K\,C + J_v\,D + J_v\,K\,C\,D\,E)^4}{L_v\,(1 + K\,C + J_v\,D + J_v\,K\,C\,D\,E)^4 + (1 + J_v + K + J_v\,K\,E)^4},\\
E_{\mathrm{K}} &= \frac{RT}{z_{\mathrm{K}}F}\ln\left(\frac{[K^+]_o}{[K^+]_i}\right).
\end{aligned}
$$

Figure 2b shows the voltage-current curve for this channel fit to experimental data (13).

The **delayed-rectifier** was one of the channels found in the chondrocyte (16–18). These usually repolarize active cells following action potentials but their role in chondrocytes are not known because chondrocytes are far more depolarised. Kv 1.4 and 1.6 (18, 19) are known to exist. Others might as well. In this work, the mathematical expression for the delayed rectifier is motivated by the ultra-rapidly rectifying potassium channel (20):

$$I_{\mathrm{K_{ur}}} = g_{\mathrm{K_{ur}}}\,a_{\mathrm{ur}}\,i_{\mathrm{ur}}\,(V - E_{\mathrm{K}}), \tag{3}$$

where i_{ur} and a_{ur} are computed as part of the solution of the ODE system defined by Equation 10, and the following expressions define quantities related to this time-dependent channel:

$$
\begin{aligned}
E_{\mathrm{K}} &= \frac{RT}{z_{\mathrm{K}}F}\ln\left(\frac{[K^+]_o}{[K^+]_i}\right),\\
a_{\mathrm{ur}_\infty} &= \frac{1}{1 + \exp(-(V_{\mathrm{m}} + 6.0)/8.6)},\\
i_{\mathrm{ur}_\infty} &= \frac{1}{1 + \exp(-(V_{\mathrm{m}} + 7.5)/10.0)) + 0.7},\\
\tau_{a_{\mathrm{ur}}} &= \frac{0.009}{1 + \exp((V + 5.0)/12.0)} + 0.0005,\\
\tau_{i_{\mathrm{ur}}} &= \frac{0.5}{1 + \exp((V + 60.0)/20.0)} + 6.
\end{aligned}
$$

Figure 2c shows the voltage-current curve for this channel fit to experimental data (13) and Figure 2d shows the time-current curve over the same period.

Pumps and exchangers

~~As for other cell types,~~ chondrocyte cell volume can be ~~modelled by a pump-leak model – a double Donnan equilibrium existing between the intracellular compartment and the extra-cellular environment~~ (3). The effective expulsion of Na^+ ions from the cell is achieved by the activity of the Na^+-K^+ ATPase, ~~and volume is maintained by altered balance of leaks and pumps to hold cell water constant~~. Due to the high $[Na^+]_o$ of their surroundings, chondrocytes are known to have a high Na^+-K^+ ATPase activity, with expression and functional activity upregulated to raised extracellular Na^+ (21).

In ~~the current~~ model, we employ the following **sodium-potassium pump** formulation from Nygren et al. (22) ~~to model this channel.~~

$$I_{NaK} = \bar{I}_{NaK}\left(\frac{[K^+]_o}{[K^+]_o + k_{NaK_K}}\right)\left(\frac{[Na^+]_i^{1.5}}{[Na^+]_i^{1.5} + k_{NaK_{Na}}^{1.5}}\right)\left(\frac{V+150}{V+200}\right) \quad (4)$$

Figure ?? shows a representative voltage-current curve for this ~~channel~~.

As in many other cell types, the **sodium-calcium exchanger** plays a key role in Ca^{2+} homeostasis in articular chondrocytes (?). In this work, we model this channel using the following mathematical expression (22):

$$I_{NaCa} = k_{NaCa}\frac{[Na^+]_i^3[Ca^{2+}]_o \exp(\frac{\gamma VF}{RT}) - [Na^+]_o^3[Ca^{2+}]_i \exp(\frac{(\gamma-1.0)VF}{RT})}{1.0 + d_{NaCa}([Na^+]_o^3[Ca^{2+}]_i + [Na^+]_i^3[Ca^{2+}]_o)} \quad (5)$$

~~Literature suggests~~ that chondrocytes possess a **sodium-hydrogen antiporter** (5, 8) which allows the cell to sense extra-cellular pH. In order to model this channel, we use the following functional form described in Cha et al. (23):

$$I_{NaH} = N_{NaH} I_{NaH_{mod}} I_{NaH_{exch}} \quad (6)$$

where,

$$
\begin{aligned}
I_{\mathrm{NaH_{mod}}} &= \frac{1}{1+(K_{\mathrm{i}}^{n_{\mathrm{H}}}/[\mathrm{H}^+]_{\mathrm{i}}^{n_{\mathrm{H}}})}, \\
t_1 &= \frac{k_1^+[\mathrm{Na}^+]_{\mathrm{o}}/K_{\mathrm{Na}}^{\mathrm{o}}}{(1+[\mathrm{Na}^+]_{\mathrm{o}}/K_{\mathrm{Na}}^{\mathrm{o}}+[\mathrm{H}^+]_{\mathrm{o}}/K_{\mathrm{H}}^{\mathrm{o}})} \\
t_2 &= \frac{k_2^+[\mathrm{H}^+]_{\mathrm{i}}/K_{\mathrm{H}}^{\mathrm{i}}}{(1+[\mathrm{Na}^+]_{\mathrm{i}}/K_{\mathrm{Na}}^{\mathrm{i}}+[\mathrm{H}^+]_{\mathrm{i}}/K_{\mathrm{H}}^{\mathrm{i}})} \\
t_3 &= \frac{k_1^-[\mathrm{Na}^+]_{\mathrm{i}}/K_{\mathrm{Na}}^{\mathrm{i}}}{(1+[\mathrm{Na}^+]_{\mathrm{i}}/K_{\mathrm{Na}}^{\mathrm{i}}+[\mathrm{H}^+]_{\mathrm{i}}/K_{\mathrm{H}}^{\mathrm{i}})} \\
t_4 &= \frac{k_2^-[\mathrm{H}^+]_{\mathrm{o}}/K_{\mathrm{H}}^{\mathrm{o}}}{(1+[\mathrm{Na}^+]_{\mathrm{o}}/K_{\mathrm{Na}}^{\mathrm{o}}+[\mathrm{H}^+]_{\mathrm{o}}/K_{\mathrm{H}}^{\mathrm{o}})}, \\
I_{\mathrm{NaH_{exch}}} &= \frac{(t_1t_2-t_3t_4)}{(t_1+t_2+t_3+t_4)}.
\end{aligned}
\tag{7}
$$

have been developed as standard

Background Leakage Currents

The model accounts for background leakage of Na^+ and K^+ through the use of time-independent channels whose mathematical expressions ~~are motivated~~ by Hodgkin and Huxley: formulation.

$$
\begin{aligned}
I_{\mathrm{Na_b}} &= \bar{g}_{\mathrm{Na_b}}(V_{\mathrm{m}}-E_{\mathrm{Na}}), \\
I_{\mathrm{K_b}} &= \bar{g}_{\mathrm{K_b}}(V_{\mathrm{m}}-E_{\mathrm{K}}),
\end{aligned}
\tag{8}
$$

~~where~~ The Nernst potentials for ~~the two species~~ are computed ~~in terms of~~ their respective ~~interior~~ and ~~exterior~~ concentrations:

Na+ and K+ based on intra- extracellular

$$
\begin{aligned}
E_{\mathrm{Na}} &= \frac{RT}{z_{\mathrm{Na}}F}\ln\left(\frac{[Na^+]_o}{[Na^+]_i}\right), \\
E_{\mathrm{K}} &= \frac{RT}{z_{\mathrm{K}}F}\ln\left(\frac{[K^+]_o}{[K^+]_i}\right).
\end{aligned}
$$

This

~~Analogously,~~ ~~the~~ model accounts for chloride leakage through a similar mathematical ~~expression~~, using

can

$$
I_{\mathrm{Cl_b}} = \bar{g}_{\mathrm{Cl_b}}(V_{\mathrm{m}}-E_{\mathrm{Cl}}), \tag{9}
$$

where

$$
E_{\mathrm{Cl}} = \frac{RT}{z_{\mathrm{Cl}}F}\ln\left(\frac{[Cl^-]_o}{[Cl^-]_i}\right)
$$

formulation

is the Nernst potential set up by the difference in Cl^- concentration inside and outside the cell.

While the above background leakage currents are mostly incorporated in the model as a means of accounting for ion transport not explicitly modelled by the previously-introduced channels, experimental studies have managed to isolate one specific chloride leakage channel in human articular chondrocytes: CFTR (12). Such channels are likely necessary for anion loss and may thus be important in regulating the RMP of the cell.

The atypical environment of the chondrocyte

Deep within cartilaginous tissue, the chondrocyte's extracellular ~~environs~~ is unique in comparison with other ~~tissue~~ types. The high number of fixed negative charges on ~~resident~~ proteoglycans attracts free cations (e.g. Na^+) and excludes free anions from the matrix. ~~With~~ this cation accumulation, water ~~is~~ osmotically ~~imbibed~~, ~~resulting~~ in lowered pH in comparison with other extracellular environments (8, 24).

As the tissue is avascular, synovial fluid supplies adult articular cartilage with small amounts of nutrients as well as oxygen, and byproducts are removed by diffusion (24, 25). Due to the ~~aforementioned~~ avascular nature of the resident tissue, chondrocytes generate ATP by substrate-level phosphorylation during anaerobic respiration, generating H^+ ions as a byproduct ~~and~~ further lowering surrounding pH (24). Mechanical loading during activity also exposes chondrocytes to profound fluctuations in their physiochemical environment (26, 27).

This atypical environment is reflected in measurements taken in tissue samples (see Table 1). Experimentally-reported values for the external concentrations of different species reveal some marked extremity in cation concentrations compared to e.g. cardiac tissue. We ~~employ~~ these extracellular concentrations in our model in concert with measured values from (13) to characterize the extracellular environment of the chondrocyte in our model.

~~Theoretical~~ model of ~~chondrocyte electrophysiology~~

In order to simplify the treatment, we assume that there are no spatial variations in these quantities of interest, allowing us to model the cell as the following set of ordinary differential equations (ODEs) in time.

	Cytoplasm	Matrix	Serum/Synovium
$[Na^+]_o$(mM)	40	240–350	140
$[K^+]_o$(mM)	120–140	7–12	5
$[Ca^{2+}]_o$(mM)	8.e-5	6–15	1.5
$[Cl^-]_o(mM)$	60–90	60–100	140
$[HCO_3^-]_o(mM)$	20	15	23
$[SO_4^{2-}]_o(mM)$	0.17	0.30	0.81
pH (mM)	7.1	6.6–6.9	7.4
Osmolarity (mOsm)	—	350–450	300

Table 1: Experimental ranges of external concentrations (8).

$$\frac{d}{dt}\begin{pmatrix} V_{\mathrm{m}} \\ [Na^+]_i \\ [\mathrm{K}^+]_i \\ [\mathrm{Ca}^{2+}]_i \\ [\mathrm{H}^+]_i \\ [\mathrm{Cl}^-]_i \\ a_{\mathrm{ur}} \\ i_{\mathrm{ur}} \end{pmatrix} = \begin{pmatrix} -I_i/C_{\mathrm{m}} \\ -(I_{\mathrm{Na_b}} + 3\,I_{\mathrm{NaK}} + 3\,I_{\mathrm{NaCa}} - I_{\mathrm{NaH}})/(v_i\,F) \\ -(I_{\mathrm{K_b}} - 2\,I_{\mathrm{NaK}} + I_{\mathrm{K_{ur}}} + I_{\mathrm{K_{2\,pore}}} + I_{\mathrm{K_{Ca-act}}})/(v_i\,F) \\ I_{\mathrm{NaCa}}/(v_i\,F) \\ -I_{\mathrm{NaH}}/(v_i\,F) \\ I_{\mathrm{Cl_b}}/(v_i\,F) \\ (a_{\mathrm{ur}_\infty} - a_{\mathrm{ur}})/\tau_{a_{\mathrm{ur}}} \\ (i_{\mathrm{ur}_\infty} - i_{\mathrm{ur}})/\tau_{i_{\mathrm{ur}}} \end{pmatrix} \tag{10}$$

where,

$$I_i = \underbrace{I_{\mathrm{K_{ur}}} + I_{\mathrm{K_{2\,pore}}} + I_{\mathrm{K_{Ca-act}}}}_{\text{Potassium currents}} + \underbrace{I_{\mathrm{NaK}} + I_{\mathrm{NaCa}} + I_{\mathrm{NaH}}}_{\text{Pumps and exchangers}} + \underbrace{I_{\mathrm{Na_b}} + I_{\mathrm{K_b}} + I_{\mathrm{Cl_b}}}_{\text{Background currents}}$$

The individual currents above are defined by Equations 2–9, and the ODE system (10) is solved for the primary vector of unknowns: V_{m}, $[\mathrm{Na}^+]_{\mathrm{i}}$, $[\mathrm{K}^+]_{\mathrm{i}}$, $[\mathrm{Ca}^{2+}]_{\mathrm{i}}$, $[\mathrm{H}^+]_{\mathrm{i}}$, $[\mathrm{Cl}^-]_{\mathrm{i}}$, a_{ur}, and i_{ur} in the time period of the numerical experiment. The initial conditions are chosen from previous calculations run to steady state. The equation system is solved using LSODE (28), and the corresponding GNU Octave code is available free and open source for anyone to use and extend (12).

Figure Legends

Figure 1.

An illustration summarising the various channels considered in the current electrophysiological model of the chondrocyte.

Figure 2.

Potassium currents which are fit to experimental values (in red) from Clark et al. (13). The external concentrations correspond to the experimental conditions: $[K^+]_o$= 5 mM, $[Na^+]_o$= 140 mM, $[Ca^{2+}]_o$= 2 mM, pH = 7.4, except for $I_{K_{2\,pore}}$, where $[K^+]_o$= 145 mM, pH = 8.5.

Figure 3.

V-I relations for the other currents. These are not fit to experimental data, but used to tune simulation results.

Figure 4.

Overall behaviour of the model when voltage is ramped from -130 mV to +90 mV in 1 s. It validates well with respect to experimental data (red) from Clark et al. (13).

Figure 5.

Time-evolution of the concentrations over 1800 s to show that the initial conditions we have chosen for the model were at steady state. The initial conditions for the concentrations used in the computations were $[Na^+]_i$= 2.814 mM, $[K^+]_i$= 121.59 mM, $[Ca^{2+}]_i$= 2.371e-06 mM, $[H^+]_i$= 6.188e-10 mM, $[Cl^-]_i$= 13.209 mM.

Figure 6

When the amount of $I_{K_{2\,pore}}$ is varied from 100% to 0% (by blocking with increasing amounts of BUP), the RMP increases. These simulations were carried out at two different values of external concentrations $[K^+]_o$= 5 mM and $[K^+]_o$= 25 mM and validates well with respect to experimental data (13, Fig. 8B).

Figure 6

Evolution of the resting membrane potential with varying external potassium concentration. Note that while it is slightly more positive than experiments, it matches the qualitative behaviour quite closely (13).

Figure 8

Relative swelling of the cell from homeostasis under different fractions of $I_{\mathrm{K_2\,pore}}$ blockage. The swollen volumes were recorded after the model was allowed to evolve for 15 s.

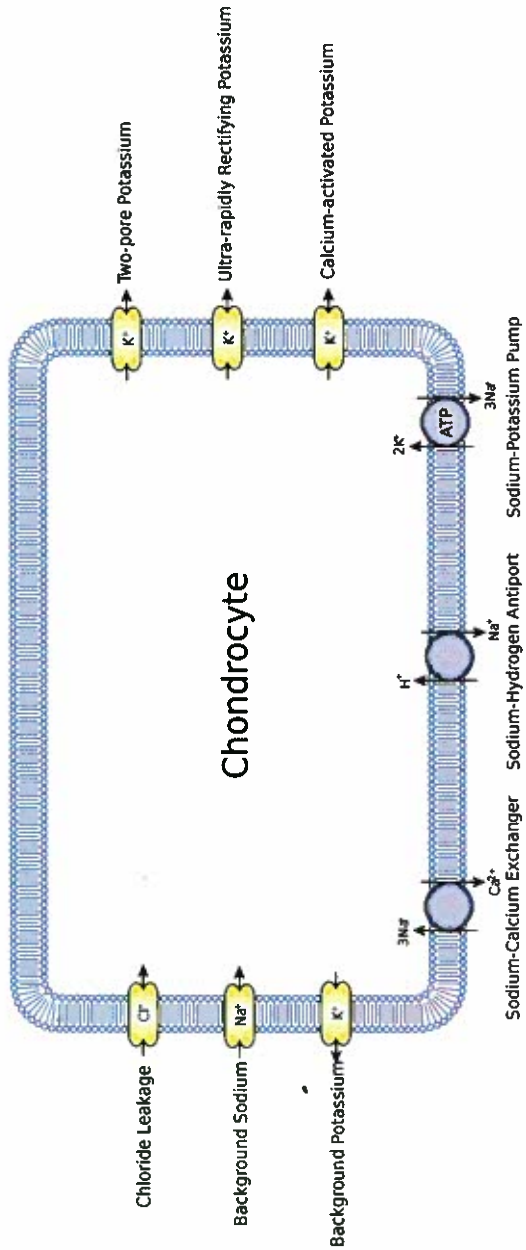

Figure 1

Orient all Figures North South

increase lettering size 2 or 3x.

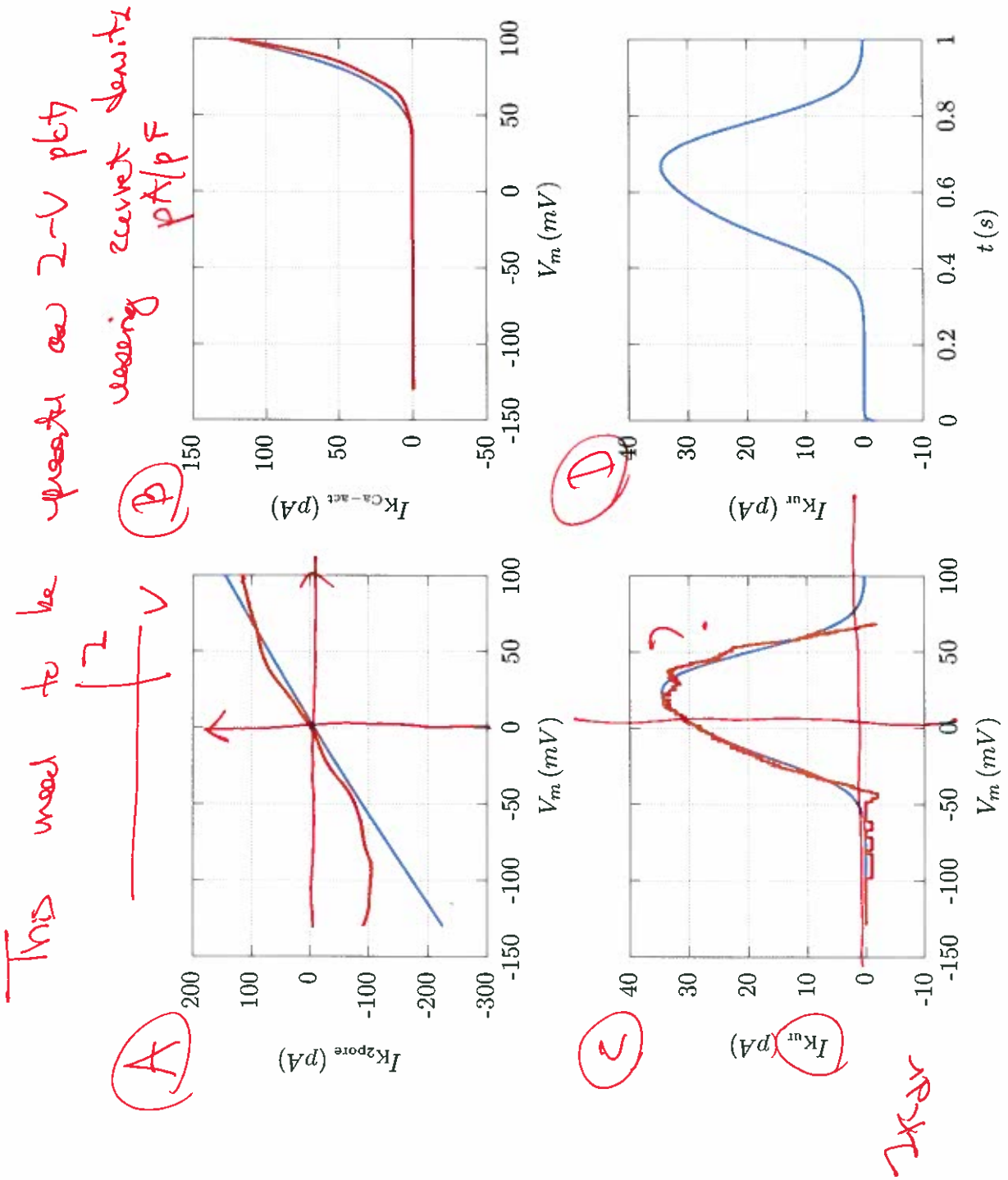

Figure 2

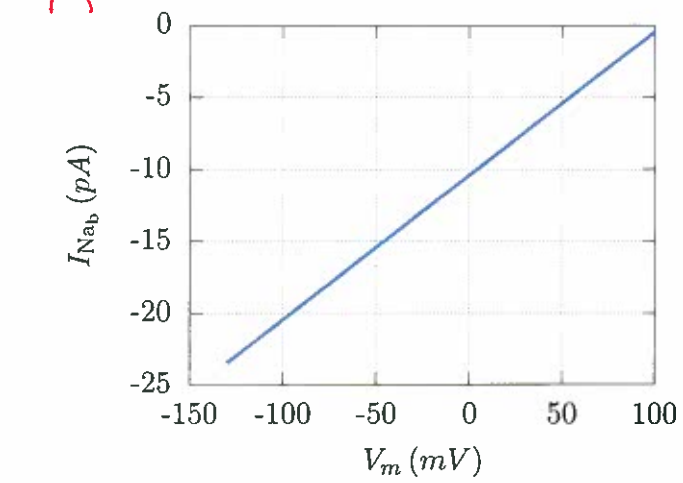
0
-5
-10
-15
-20
-25
I_{Na_b} (pA)
-150 -100 -50 0 50 100
V_m (mV)

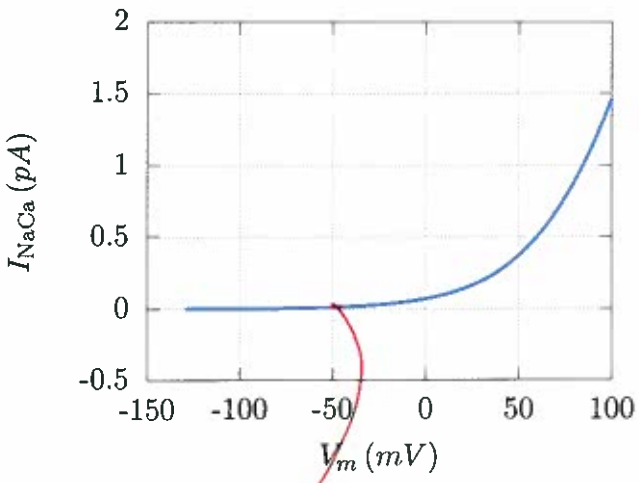
2
1.5
1
0.5
0
-0.5
I_{NaCa} (pA)
-150 -100 -50 0 50 100
V_m (mV)

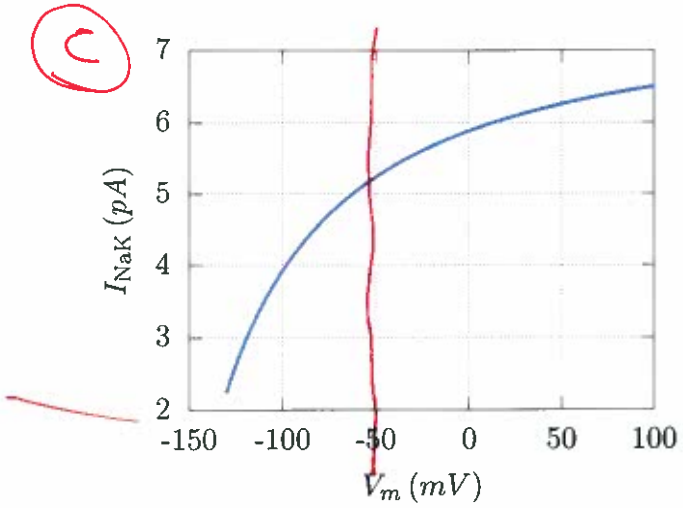
7
6
5
4
3
2
I_{NaK} (pA)
-150 -100 -50 0 50 100
V_m (mV)

Figure 3

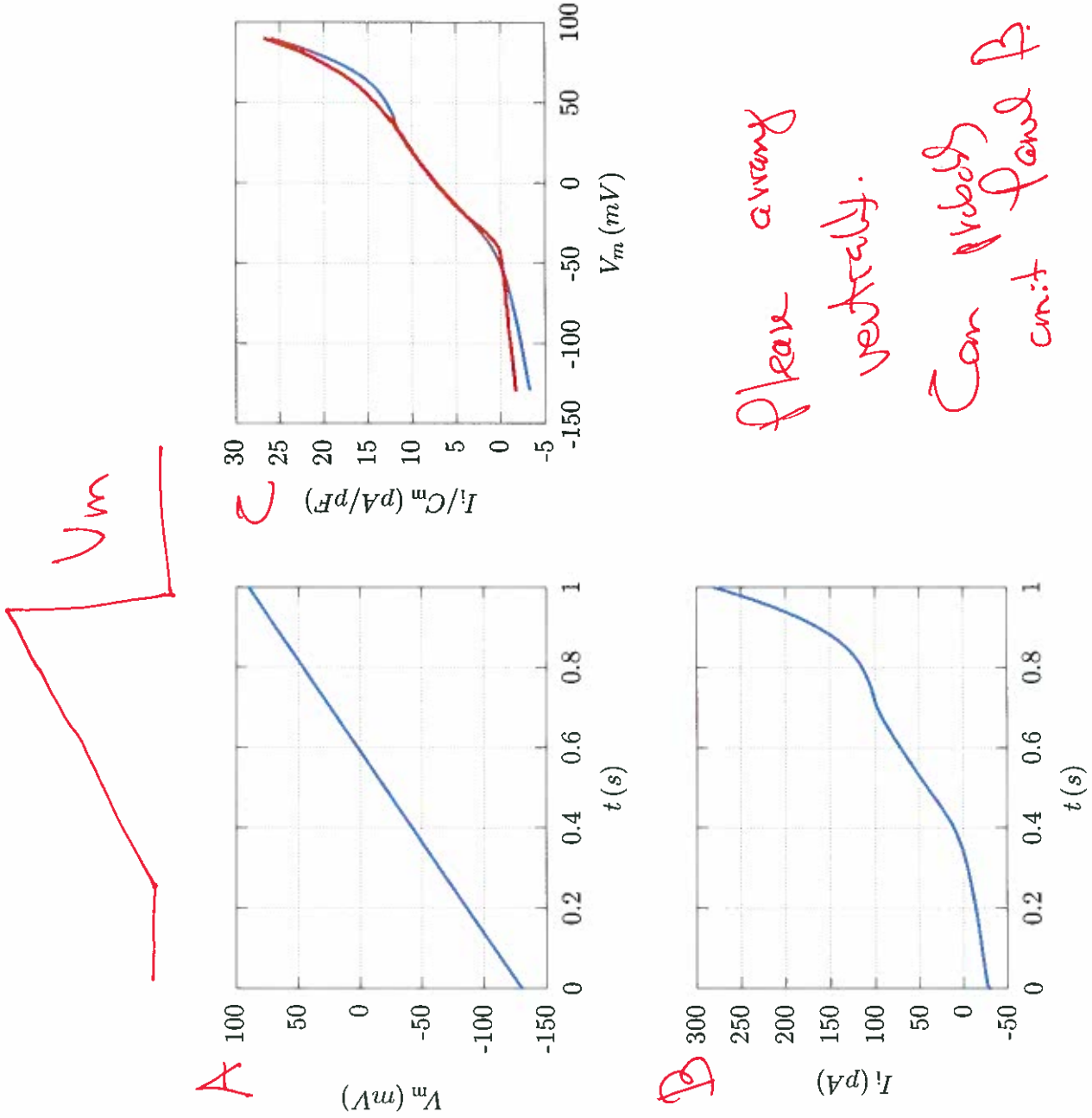

Figure 4

This important validation can be moved to an Appendix

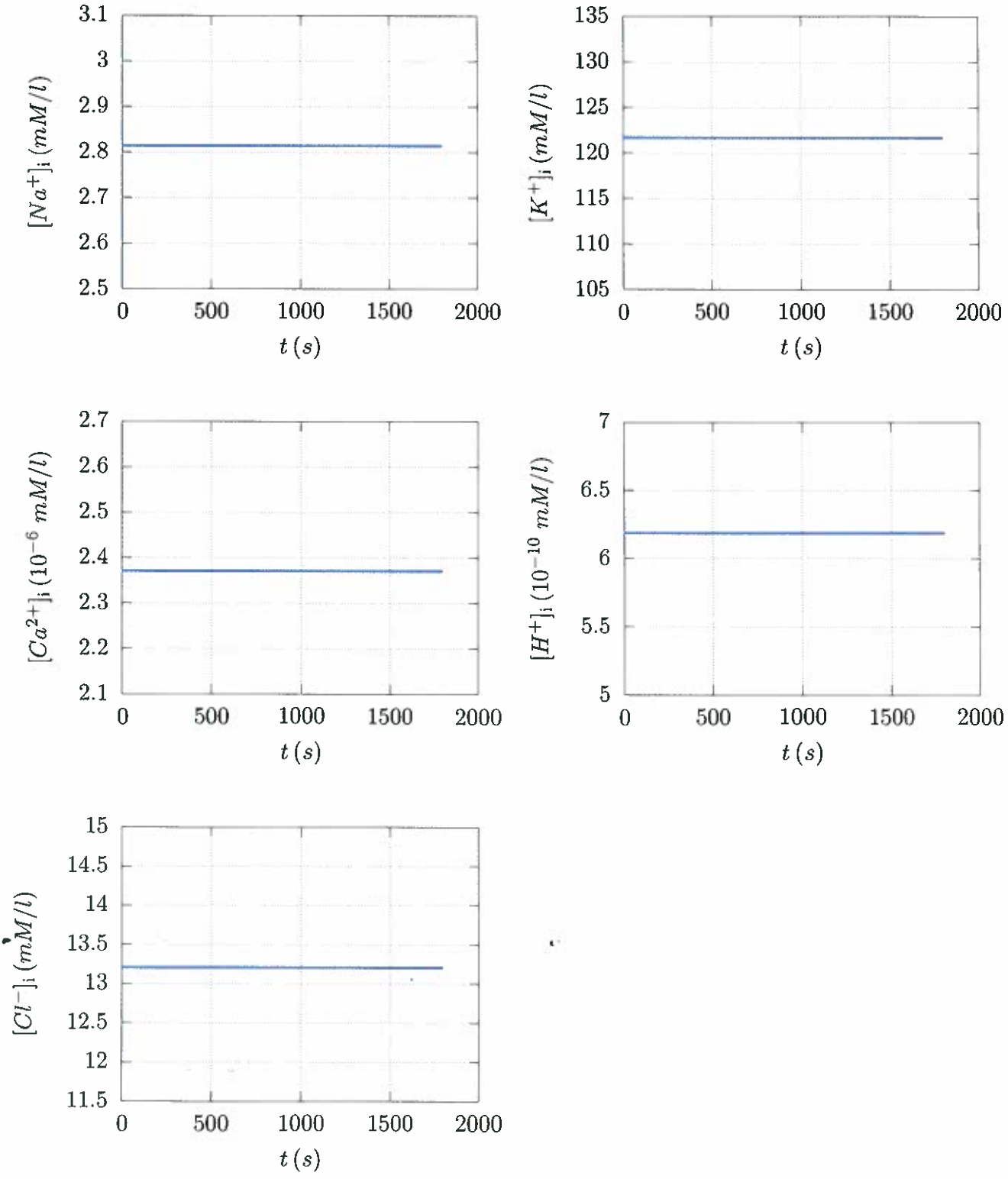

Figure 5

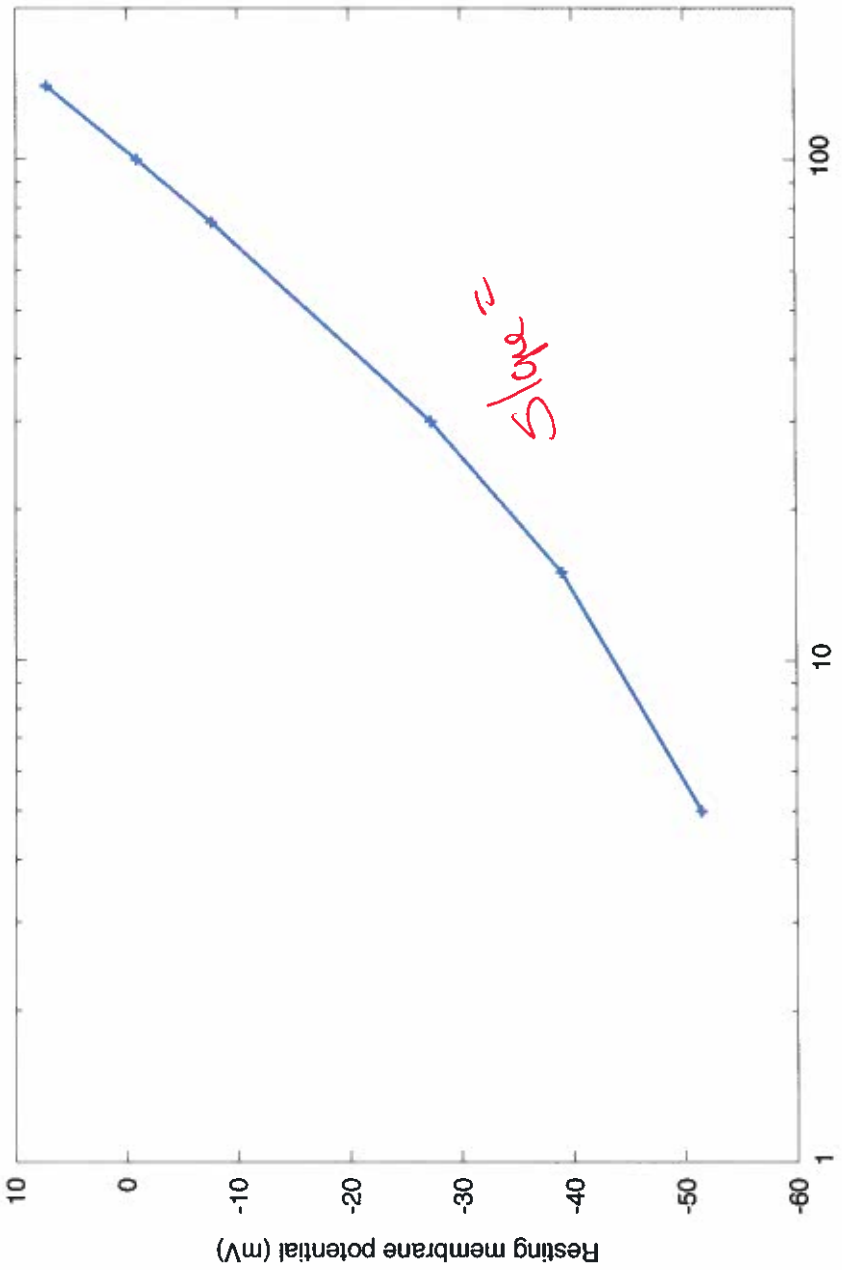
Resting membrane potential (mV)
10
0
-10
-20
-30
-40
-50
-60
1
10
100
$[K^+]_o$ (mM)

Figure 6

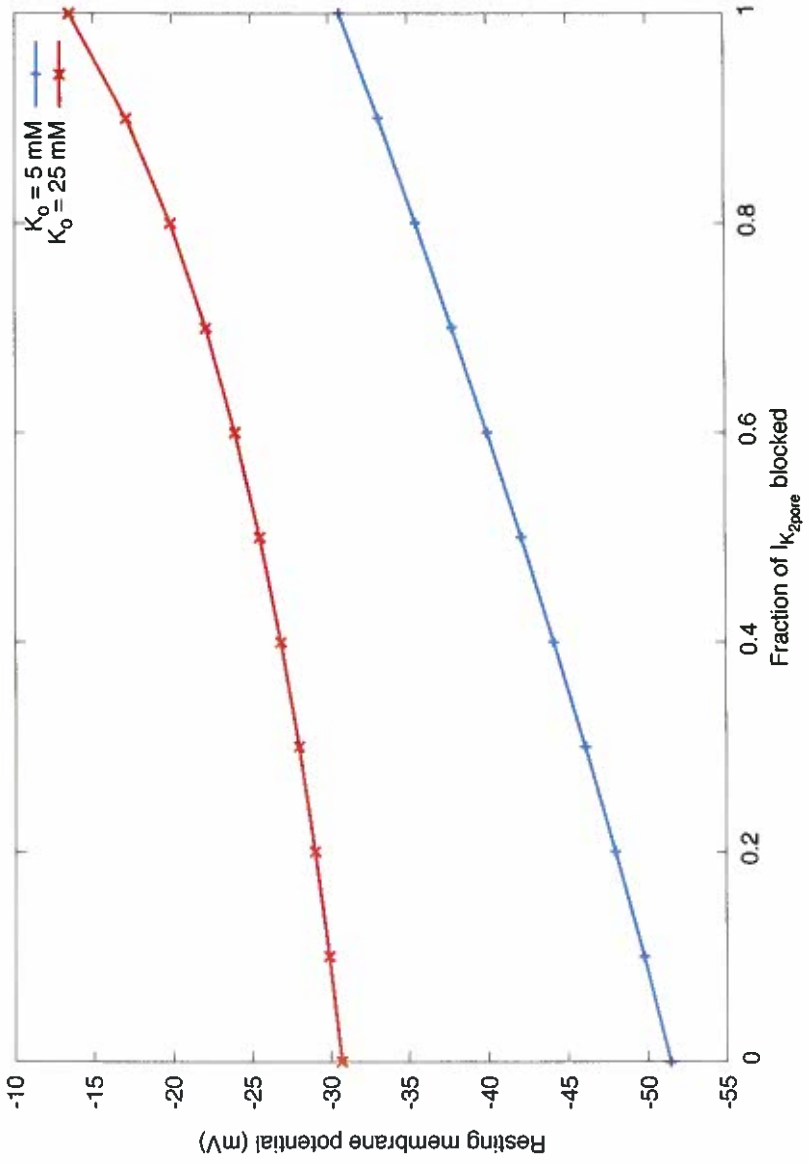
K_o = 5 mM
K_o = 25 mM
Resting membrane potential (mV)
-10
-15
-20
-25
-30
-35
-40
-45
-50
-55
0
0.2
0.4
0.6
0.8
1
Fraction of I_{K2pore} blocked

Figure 7

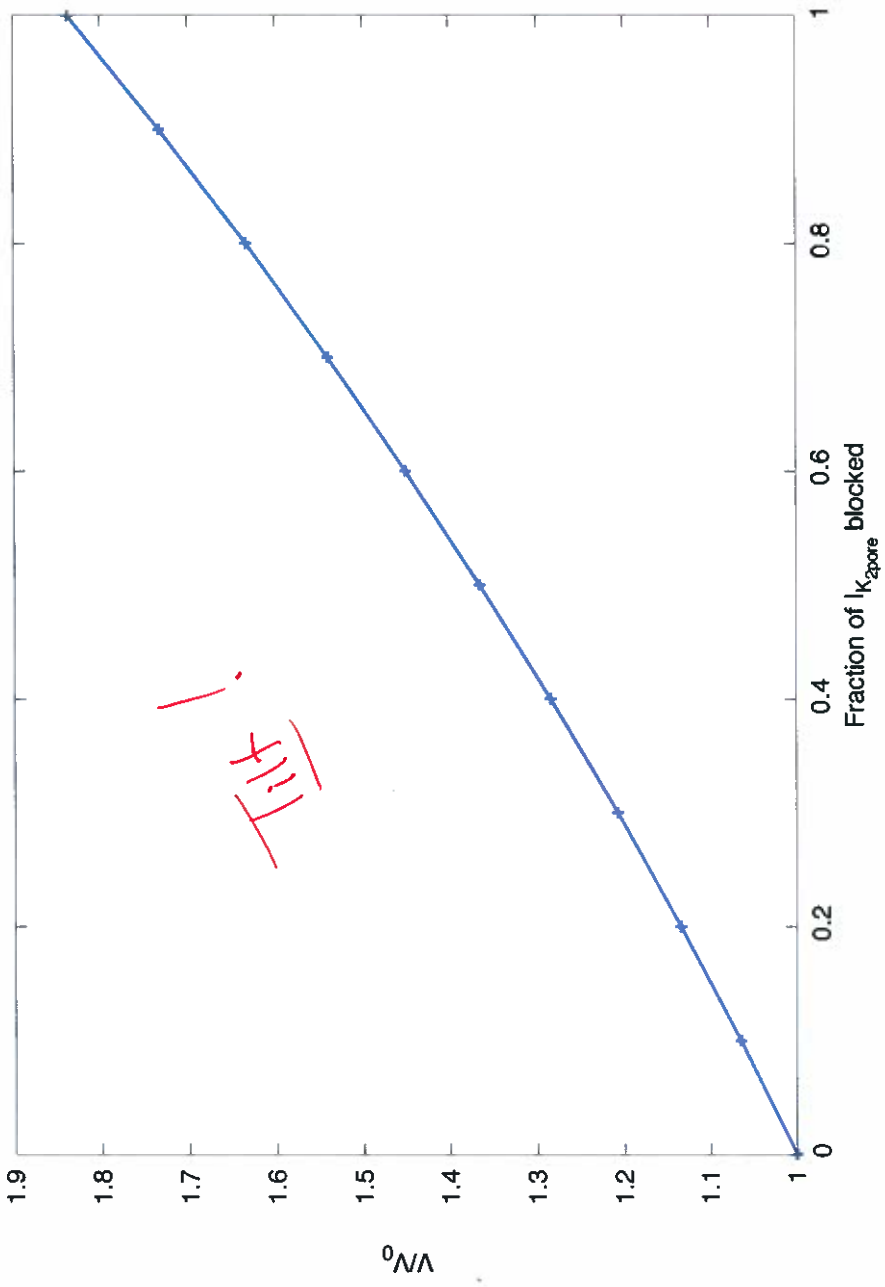
V/V0
1.9
1.8
1.7
1.6
1.5
1.4
1.3
1.2
1.1
1
0
0.2
0.4
0.6
0.8
1
Fraction of $I_{K_{2pore}}$ blocked

Figure 8

Voltage-gated calcium channels: T, L-type VGCC found in some cartilage. Others refute. Supposedly, aggrecan and collagen synthesis induced by electrical stimulation relies on this channel. We will claim not important for RMP, just tissue growth, and thus we do not consider.

Epithelial sodium channels (EnaC): Not clear what role this plays in chondrocytes, though it has been identified. People speculate it has something to do with mechanotransduction $\rightarrow$ contributes to RMP. It is perhaps defective during osteoarthritis. We will point out we do not look at this as it pertains to mechanics.

Aquaporin channels: AQP or some other mechanism for transport of water seems super important to the functioning of the cell. Studies show loss of volume regulation with inhibition of AQP. But we will point out that we do not model it because it pertains to mechanics.

NMDA channels: This is an excitatory neuro-transmitter receptor. It is possibly linked to mechanotransduction.

References

1. Poole, C. A., 1997. Articular cartilage chondrons: form, function and failure. *J. Anat.* 191:1–13.

2. Mankin, H. J., 1982. The response of articular cartilage to mechanical injury. *J. Bone Joint Surg. Am.* 64:460–466.

3. Stockwell, R. A., 1991. Cartilage failure in osteoarthritis: Relevance of normal structure and function. A review. *Clin. Anat.* 4:161–191.

4. Carney, S. L., and H. Muir, 1988. The structure and function of cartilage proteoglycans. *Physiol. Rev.* 68:858–910.

5. Hall, A. C., E. R. Horwitz, and R. J. Wilkins, 1996. The cellular physiology of articular cartilage. *Exp. Physiol.* 81:535–545.

6. Buckwalter, J. A., and H. J. Mankin, 1998. Articular cartilage: Tissue design and chondrocyte-matrix interactions. *Instr. Course Lect.* 47:477–486.

7. Edwards, J. C., L. S. Wilkinson, H. M. Jones, P. Soothill, K. J. Henderson, J. G. Worrall, and A. A. Pitsillides, 1994. The formation of human synovial joint cavities: A possible role for hyaluronan and CD44 in altered interzone cohesion. *J. Anat.* 185:355–367.

8. Wilkins, R. J., J. A. Browning, and J. C. Ellory, 2000. Surviving in a Matrix: Membrane Transport in Articular Chondrocytes. *J. Membrane Biol.* 177:95–108.

9. Fassbender, H. G., 1987. Role of chondrocytes in the development of osteoarthritis. *Am. J. Med.* 83:17–24.

10. Lewis, R., K. E. Asplin, G. Bruce, C. Dart, A. Mobasheri, and R. Barrett-Jolley, 2011. The role of the membrane potential in chondrocyte volume regulation. *J. Cell. Physiol.* xx:mm–nn.

11. Chu, C. R., N. J. Izzo, N. E. Papas, and F. H. Fu, 2006. In Vitro Exposure to 0.5% Bupivacaine Is Cytotoxic to Bovine Articular Chondrocytes. *J. Arthroscopy* 22:693–699.

12. Unknown, A., yyyy. This is an unknown article. *J. Unknown* xx:mm–nn.

13. Clark, R. B., C. Kondo, and W. R. Giles, 2011. Two-pore K^+ channels contribute to membrane potential of isolated human articular chondrocytes. *J. Physiol.* xx:mm–nn.

14. Barrett-Jolley, R., R. Lewis, R. Fallman, and A. Mobasheri, 2010. The emerging chondrocyte channelome. *Front. Physiol.* 1:mm–nn.

15. Horrigan, F. T., and R. W. Aldrich, 2002. Coupling between Voltage Sensor Activation, Ca^{2+} Binding and Channel Opening in Large Conductance (BK) Potassium Channels. *J. Gen. Physiol.* 120:267–305.

16. Walsh, K. B., S. D. Cannon, and R. E. Wuthier, 1992. Characterization of a delayed rectifier potassium current in chicken growth plate chondrocytes. *Am. J. Physiol.* 262:C1335–C1340.

17. Sugimoto, T., M. Yoshino, M. Nagao, S. Ishii, and H. Yabu, 1996. Voltage-Gated Ionic Channels in Cultured Rabbit Articular Chondrocytes. *Comp. Biochem. Physiol.* 115C:223–232.

18. Mobasheri, A., T. C. Gent, M. D. Womack, S. D. Carter, P. D. Clegg, and R. Barrett-Jolley, 2005. Quantitative analysis of voltage-gated potassium currents from primary equine (Equus caballus) and elephant (Loxodonta africana) articular chondrocytes. *Am. J. Physiol. Regul. Integr. Comp. Physiol.* 289:R172–R180.

19. Clark, R. B., N. Hatano, C. Kondo, D. D. Belke, B. S. Brown, S. Kumar, B. J. Votta, and W. R. Giles, 2010. Voltage-gated K+ currents in mouse

articular chondrocytes regulate membrane potential. *Channels* 4:179–191.

20. Maleckar, M. M., J. L. Greenstein, W. R. Giles, and N. A. Trayanova, 2009. K^+ current changes account for the rate dependence of the action potential in the human atrial myocyte. *Am. J. Physiol Heart Circ. Physiol.* 297:1398–1410.

21. Mobasheri, A., R. J. Errington, S. Golding, A. C. Hall, and J. P. Urban, 1997. Characterization of the Na+, K+-ATPase in isolated bovine articular chondrocytes; molecular evidence for multiple alpha and beta isoforms. *Cell Biol. Int.* 21:201–212.

22. Nygren, A., C. Fiset, L. Firek, J. W. Clark, D. S. Lindblad, R. B. Clark, and W. R. Giles, 1998. Mathematical Model of an Adult Human Atrial Cell: The Role of K^+ Currents in Repolarization. *Circ. Res.* 82:63–81.

23. Cha, C. Y., C. Oka, Y. E. Earm, S. Wakabayashi, and A. Noma, 2009. A Model of Na^+/H^+ Exchanger and Its Central Role in Regulation of pH and Na^+ in Cardiac Myocytes. *Biophys. J.* 97:2674–2683.

24. Lee, R. B., and J. P. Urban, 1997. Evidence for a negative Pasteur effect in articular cartilage. *Biochem. J.* 321:95–102.

25. Otte, P., 1991. Basic cell metabolism of articular cartilage. Manometric studies. *Z. Rheumatol.* 50:304–312.

26. Mow, V. C., C. C. Wang, and C. T. Hung, 1999. The extracellular matrix, interstitial fluid and ions as a mechanical signal transducer in articular cartilage. *Osteoarthr. Cartil.* 7:41–58.

27. Urban, J. P., 1994. The chondrocyte: A cell under pressure. *Br. J. Rheumatol.* 33:901–908.

28. Radhakrishnan, K., and A. C. Hindmarsh, 1993. Description and use of LSODE, the Livermore Solver for Ordinary Differential Equations. Technical Report UCRL-ID-113855, Lawrence Livermore National Laboratory.

29. Dart, C., and N. B. Standen, 1994. Hypoxia induces a potassium current in smooth muscle cells isolated from the porcine coronary artery. *J. Physiol.* 477:P85–P86.

30. Mobasheri, A., T. C. Gent, A. I. Nash, M. D. Womack, C. A. Moskaluk, and R. Barrett-Jolley, 2007. Evidence for functional ATP-sensitive (K(ATP)) potassium channels in human and equine articular chondrocytes. *Osteoarthr. Cartil.* 15:1–8.